Journal of Volcanology and Geothermal Research, 55 (1993) 225–238
Elsevier Science Publishers B.V., Amsterdam

Giant tuff cone and 12-km-wide associated caldera at Ambrym Volcano (Vanuatu, New Hebrides Arc)

Claude Robin, Jean-Philippe Eissen* and Michel Monzier
UR 1F, ORSTOM, BP A5, Noumea, New Caledonia

(Received April 9, 1992; revised version accepted September 1, 1992)

ABSTRACT

Robin, C., Eissen, J.-P. and Monzier, M., 1993. Giant tuff cone and 12-km-wide associated caldera at Ambrym Volcano (Vanuatu, New Hebrides Arc). *J. Volcanol. Geotherm. Res.*, 55: 225–238.

Ambrym, in the New Hebrides arc, has been considered as an effusive, basaltic volcano. The present paper discusses the general structure of this edifice, which consists of a basal shield volcano topped by an exceptionally large tuff cone surrounding a 12-km-wide summit caldera. Dacitic pyroclastic flow deposits are exposed in the lower part of the tuff series; they grade upward into composite sequences of bedded surtseyan-type hyaloclastites, ash flow deposits, and fallout tephra which are essentially basaltic in composition, in such a way that the tuff cone may be considered as mainly basaltic.

The relationship between the eruption of pyroclastics and the collapse event precludes a classical model of caldera formation at a basaltic volcano in which "quiet" subsidence (i.e. Kilauea type) is the dominant mechanism. Interpretation of the tuff series implies intervention of external water and suggests both explosive and collapse mechanisms. A model of caldera formation which assumes an enlargement of the ring fracture during a first plinian and dacitic, then essentially hydrobasaltic eruption is proposed.

Introduction

Ash flows of gas-rich differentiated material emitted during major Plinian eruptions are typically related to calderas at large explosive volcanoes and to calderas of the Valles type, whereas rapid drainage of basaltic lava flows with subordinate tephra is responsible for caldera subsidence in Hawaiian-type volcanoes. In addition, bedded hyaloclastites are commonly associated with craters and calderas from seamounts, although the question of genetic links between these structures and their formation remains unanswered (Batiza et al., 1984).

Ambrym (168°08′E; 16°15′S), the most voluminous active volcano in the New Hebrides, is a 35×50-km-wide basaltic volcano, about 1800 m high relative to the nearby sea bottom (Chase and Seekins, 1988) (Fig. 1). The main cone is crowned by a circular, 12-km-diameter caldera with a continuous scarp a few tens of meters to 450 m high (Fig. 2). Post-caldera volcanics, dominantly from the Marum and the Benbow intra-caldera cones, have partly filled the depression. Post-caldera scoria cones and lava flows also occur outside the caldera on the slopes of the edifice, along fissures oriented N 105°E (Fig. 2).

Despite its association with a basaltic volcano, the Ambrym caldera has a size similar to those of calderas related to large Plinian ignimbrite-forming eruptions. MacCall et al. (1970) stressed that transformation from pre-caldera to post-caldera eruptivity at Ambrym is not marked by any unusual type of deposit or any clear break in the eruptive sequence.

*Present address: Centre ORSTOM, BP 70, 29280 Plouzané, France.

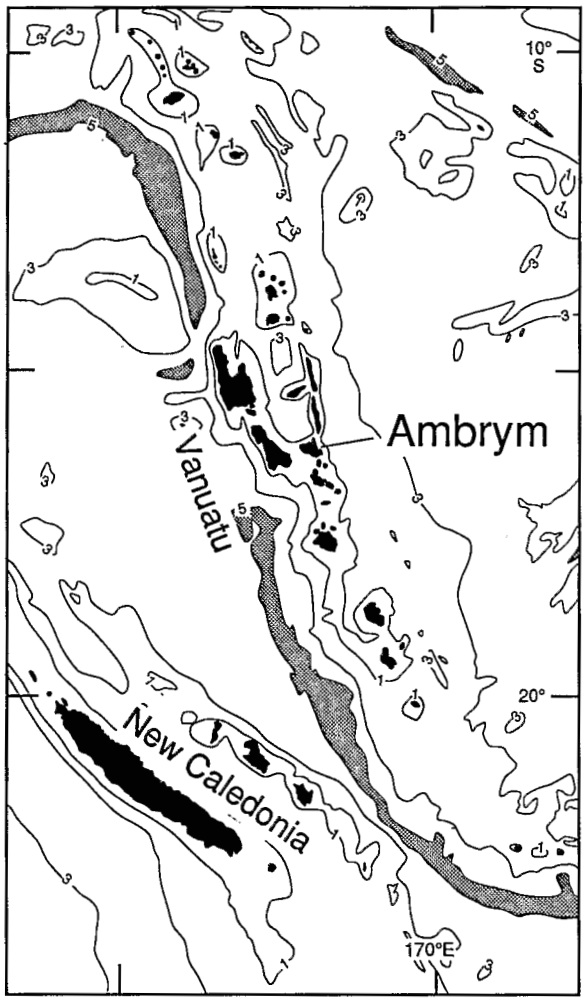

Fig. 1. Location of Ambrym (Vanuatu) in the New Hebrides island arc. The trench is represented by the shaded zone.

These authors postulate that the caldera was formed by quiet subsidence accompanied by minor eruptions of scoria lapilli, i.e. following the Hawaiian model. This is also implicit in the stratigraphy proposed by Macfarlane (1976).

The discovery of dacitic ash-and-pumice flow deposits on the lower flanks of the volcano, and of a subsequent voluminous series of mainly basaltic hyaloclastites which constitute an exceptionally large tuff cone around the caldera, allowed us to reconsider the problem of the caldera formation. The present paper emphasizes the complex association between the caldera and this tuff cone. Since such a structure is not explained by the mechanisms of caldera formation generally proposed for basaltic edifices, a tentative model based on the interpretation of the tuff series is proposed.

Main volcanic sequences

Basal edifice

The oldest subaerial volcanics are ankaramitic lava flows and pyroclastic deposits exposed in the northern part of the island. In the main cone, pre-caldera lava flows crop out on the south, northwest and east sides along the seashore or very close to the coast (Quantin, 1978). They are commonly porphyritic, low viscosity basalts (pahoehoe type), which constitute a basal shield volcano with very gentle slopes (2–3°).

The Ambrym Pyroclastic Series

A series of bedded tuffs (the Ambrym Pyroclastic Series: APS, Fig. 3) overlies the basal shield volcano and constitutes most of the volume of the truncated cone up to the caldera rim. The importance of these tuffs in the volcanological development of the edifice was not revealed by previous work. Numerous layers have brown colours, which makes them easy to distinguish from the overlying post-caldera grey ash and lapilli fallout deposits. Deposits of the APS have been observed as far as the western end of the island, 15 km from the caldera margin. No interruption (erosional discordance or buried soil) has been observed in these pyroclastic deposits and despite extensive erosion of the flanks of the cone, no lava flows are included in this series. We also emphasize that the scarce lava flows exposed on the upper slopes of the cone are post-caldera basalts that have overflowed the caldera rim, i.e. they are not interbedded with the pyroclas-

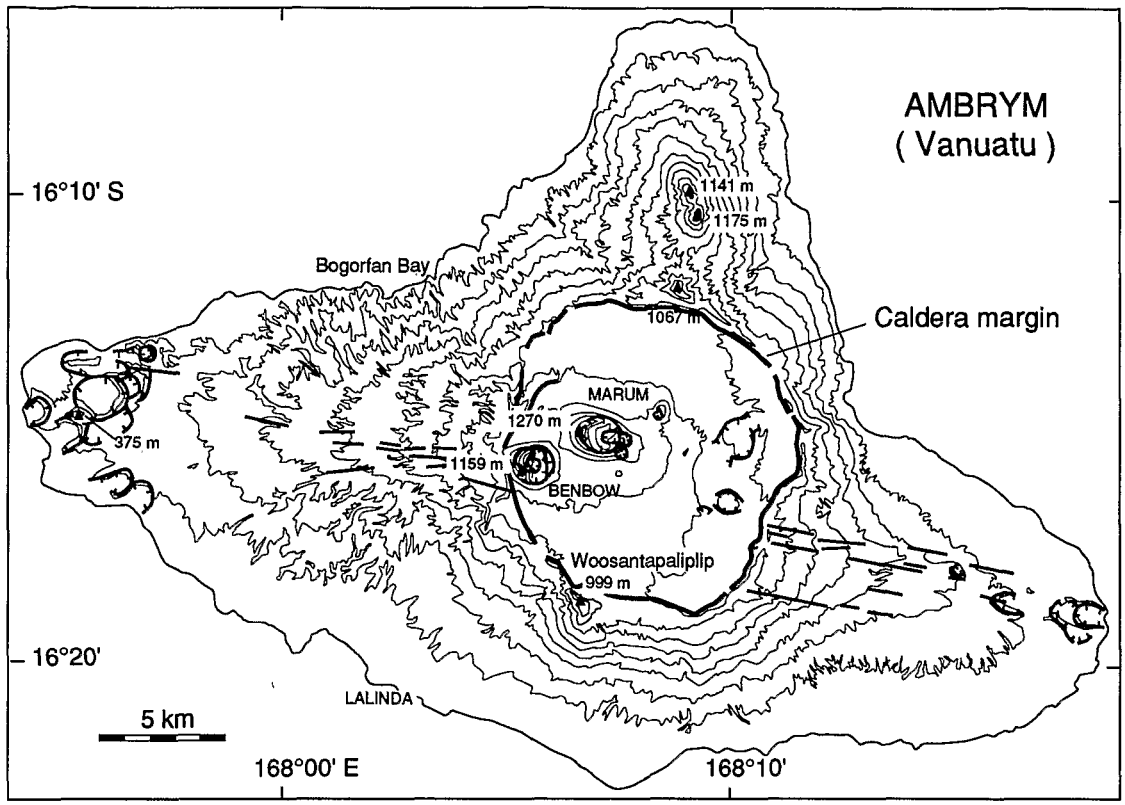

Fig. 2. Topographic map of Ambrym island. In bold, the main volcanic features (caldera, cones, maars, fissures). Contour interval, 100 m.

tic series. In addition, the only lava flow related to the caldera-forming event is a thick basaltic andesite lava flow on the NW flank which overlies the APS (see below). These field data are corroborated by careful aerial observations of the cone flanks.

Four sequences of pyroclastic deposits comprise the Ambrym Pyroclastic Series (I to IV, Fig. 3). Since this paper deals with the structure of the volcano, only the main textural features and chemical characteristics, based on microscopic and SEM observations, 64 ICP-ES whole-rock analyses and 137 microprobe analyses of vitric clasts, are reported here together with the stratigraphy. Exhaustive study of the APS is in progress and will be presented in another paper. In the following section, the term pyroclastic flow deposit is used for all flow deposits with less than 50% ash and with variable contents of lapilli-sized dense juvenile clasts, scoria and pumice, and xenoliths. The term ash flow deposit is used only for fine deposits essentially made of ash (at least 50%, commonly more than 70%).

Sequence I. Locally, on the north coast, a ≈60-m-thick lower sequence of pyroclastic flow deposits (I, Fig. 3) fills topographic depressions on the basal shield edifice. This sequence, dacitic in composition (column D, table 1), consists mainly of six sub-horizontal indurated massive units of coarse ash and medium grained lapilli (≈50%), pumice (≈15%), cauliflower bombs and glassy clasts (≈15%),

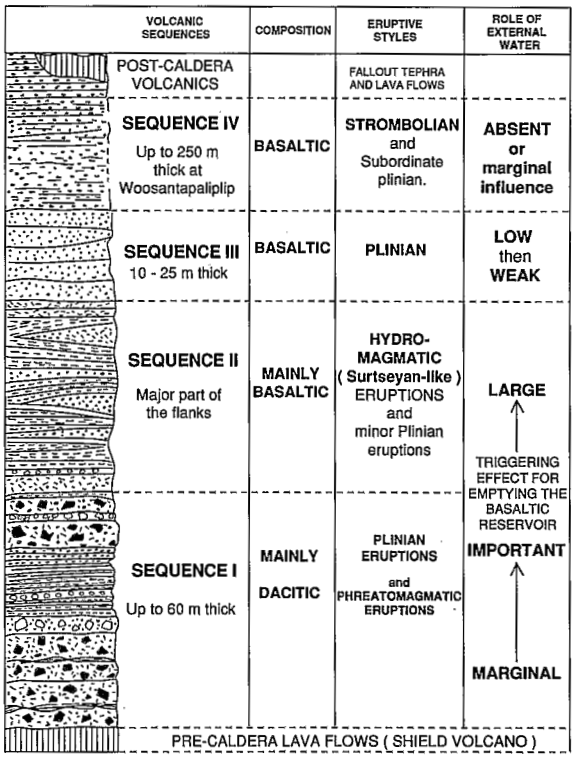

Fig. 3. Composite section of the Ambrym Pyroclastic Series (APS).

and abundant basaltic accidental clasts (≈20%). This sequence (Fig. 4A, B) also includes pumice-rich layers, surge deposits and two massive block-rich layers, respectively 5–6 and 4 m thick. An 8–10-m-thick sequence of fallout ash layers bearing abundant accretionary lapilli (Fig. 4C) occurs in the middle of the section and indicates that two major pyroclastic flow events occurred. Base surge deposits, accretionary lapilli and poorly vesiculated cauliflower bombs — interpreted as quenched juvenile material (Fisher and Schmincke, 1984)— are evidence of phreatomagmatic processes during the eruption of sequence I.

Sequence II. The deposits of sequence I grade upward into a thick sequence of well-bedded, sometimes well-sorted, laterally continuous layers of vitric tuffs (sequence II, Figs. 3 and 5A,B). The continuous beds are generally less than 3 m thick (commonly 30 cm to 1 m) and form thick deposits with intercalated lenses of agglomerates, some in excess of 8 m. Two dominant facies occur: (a) thin and coarse ash including quenched glass fragments and accretionary lapilli; and (b) agglomerates of vitric clasts and shards in a granular sideromelane matrix which also includes basaltic lithics from the basement. The sideromelane matrix is sometimes palagonitized and the vitric fragments are commonly aligned parallel to the beds. Typical shapes of the juvenile clasts are:

(1) Light-brown basaltic blocky or platy fragments (0.5–5 mm in size; analysis G, Table 1), aphyric and non-vesicular, with cracks due to quenching (up to 20% of some beds).

(2) Dark-brown to opaque basaltic glass fragments, with a low vesicularity (0 to 10 %), which can represent the major part of the matrix.

(3) Irregularly shaped, translucent basaltic or basic andesitic vitric clasts which are mainly incipiently or poorly vesicular (5 to 40 %) following the Houghton and Wilson classification (1989) but show a broad vesicularity range (up to 70 %). These clasts bear plagioclase and clinopyroxene phenocrysts, and make up to 50 % of some beds as coarse ash or lapilli.

(4) Glassy andesitic to dacitic angular fragments, also showing various degrees of vesicularity. Different types of shapes occur in the same sample; all the juvenile particles show signs of shattering, induced by the interaction with water.

Ash flow deposits are interbedded with these deposits in the upper part of the sequence. Dense vegetation, which covers the flanks of the cone, makes an estimate of the total thickness difficult; nevertheless, observations in deep gullies suggest that this sequence is very thick, at least 200 m if one considers the elevation of the slopes and the dips. Continuous exposures as thick as 50 m have been observed.

Sequence III. The following sequence (III, Fig.

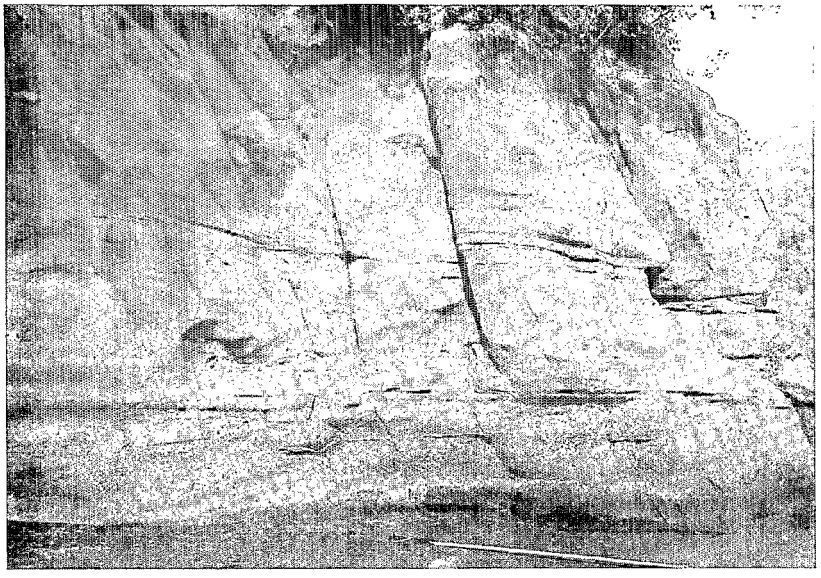

A

B

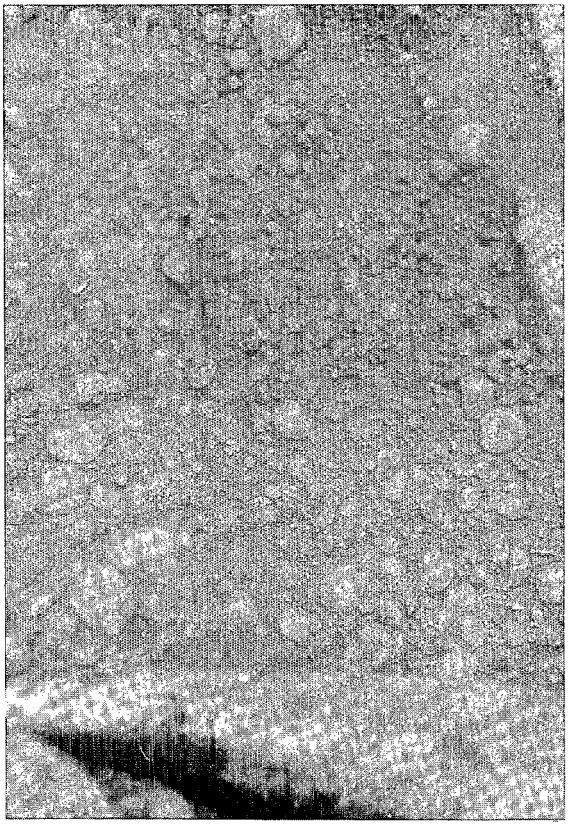

C

Fig. 4. (A) Indurated dacitic ash- and pumice flow deposits from the lower sequence of APS, north coast of Ambrym. Note the 50-cm size bomb (vitric juvenile magma). (B) Vitric-clast-rich layer from the lower dacitic sequence. (C) Fallout accretionary lapilli layer from middle part of sequence I.

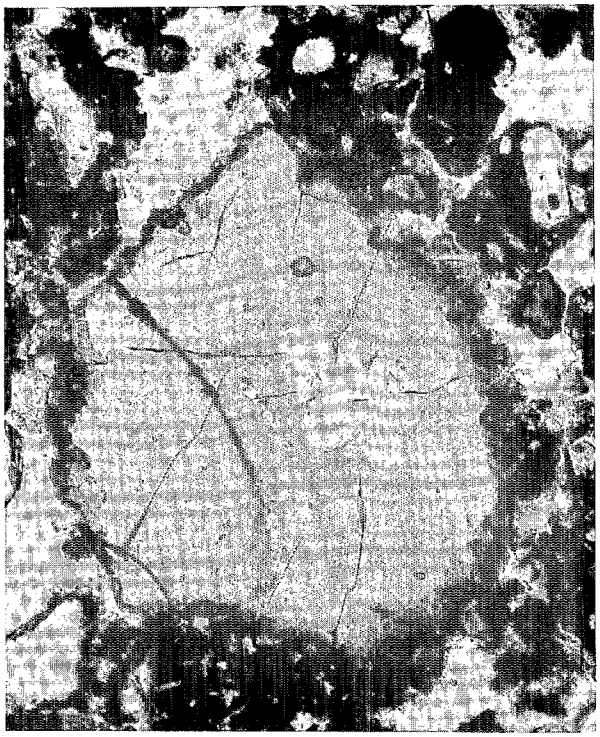

A

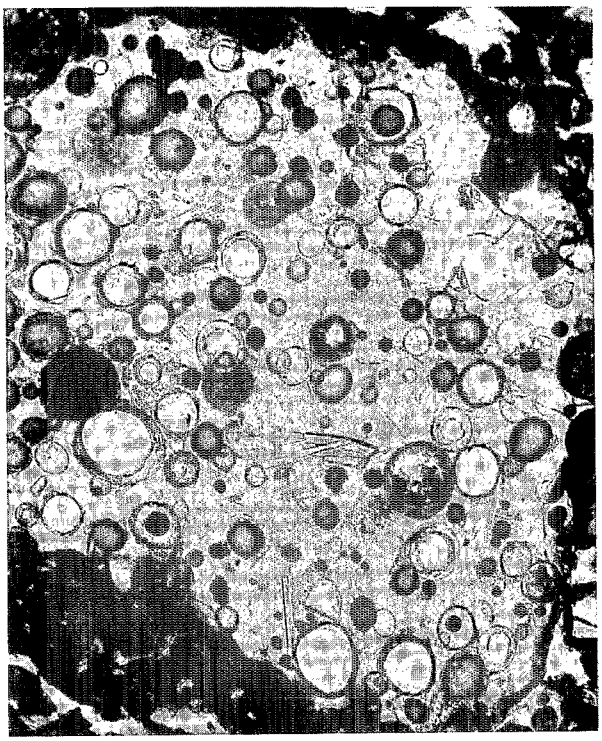

B

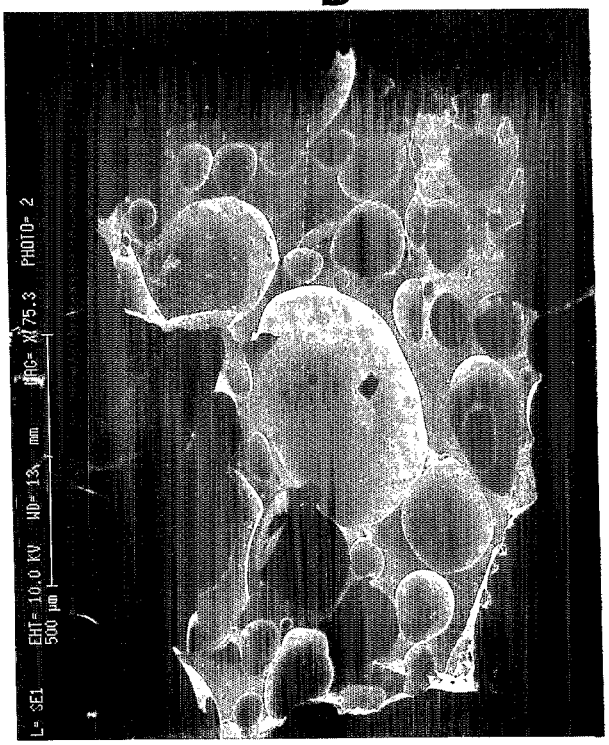

C

TABLE 1

Selected whole-rock analyses from Ambrym volcano (ICP-ES method; analyst Jo Cotten, Université de Bretagne Occidentale)

	A	B	C	D	E	F	G	H	I	J	K
	Pre-caldera lava flows			Syn-caldera pyroclastic products (APS)					Post-caldera lava flows		
	AMB72	AMB32	AMB36	AMB60	CAMB39A	AMB6012	AMB39	BAMB65	AMB20	AMB26	AMB8
SiO_2	48.50	49.30	52.30	63.50	55.00	54.10	49.60	49.40	49.80	50.75	50.40
TiO_2	0.80	0.68	0.98	0.54	0.77	0.79	0.90	0.78	0.85	0.96	0.93
Al_2O_3	14.75	18.68	16.45	14.75	15.82	16.42	15.89	17.60	15.94	15.90	15.90
Fe_2O_3	10.70	10.43	10.61	7.59	9.83	11.61	12.41	12.07	12.48	12.90	12.54
MnO	0.19	0.18	0.18	0.21	0.19	0.22	0.21	0.20	0.21	0.23	0.22
MgO	10.16	4.65	4.36	1.36	3.60	3.90	4.80	4.53	5.70	4.66	4.90
CaO	12.50	11.96	8.67	4.35	7.40	8.58	9.34	10.55	11.10	9.80	10.00
Na_2O	2.06	2.37	3.22	4.37	3.29	3.15	2.78	2.40	2.52	2.80	2.74
K_2O	0.64	1.20	2.52	2.65	2.90	1.28	1.75	0.98	1.62	1.99	1.90
P_2O_5	0.19	0.23	0.42	0.19	0.28	0.25	0.32	0.22	0.30	0.35	0.34
LOI 1050°C	−0.29	0.02	−0.08	0.54	1.53	−0.03	2.29	0.70	−0.59	−0.41	−0.59
	100.20	99.70	99.63	100.05	100.61	100.27	100.29	99.43	99.93	99.93	99.28
Rb	11	19	48	51	54	24	31	19	28	35	34
Ba	418	287	480	725	522	390	358	151	342	407	393
Nb	1.00	1.35	3.40	3.75	4.50	1.95	2.70	1.60	2.35	2.30	2.60
La	4.2	7.7	12.8	15.8	13.5	8.3	10.3	7.8	9.2	11.0	11.3
Sr	304	578	638	288	488	418	572	482	588	618	615
Nd	7.5	11.0	17.5	19.0	17.5	12.0	15.0	11.0	12.8	15.0	15.5
Zr	44	51	93	142	112	68	69	51	60	76	73
Eu	0.85	0.95	1.25	1.30	1.10	1.20	1.25	1.05	0.95	1.20	1.30
Dy	2.9	2.7	3.5	6.1	4.0	3.9	3.4	3.1	3.1	3.9	3.7
Y	16.0	16.0	21.0	41.0	24.0	23.5	20.5	18.5	17.0	22.0	21.0
Er	1.60	1.50	2.10	4.10	2.00	2.90	1.70	1.60	1.70	2.30	2.50
Yb	1.57	1.42	1.87	4.07	2.27	2.52	1.77	1.70	1.60	1.97	1.92
V	279	284	360	70	245	299	330	335	340	375	350
Cr	381	65	21	31	59	5	155	56	51	10	15
Co	49	36	32	12	29	32	41	35	45	41	40
Ni	101	27	34	17	20	13	100	38	35	24	28
Sc	43	32	24	17	23	29	29	31	32	30	32

A: ankaramitic basalt from the ancient edifice. B and C: two porphyritic basalts from the basal shield volcano. D to H: syn-caldera pyroclastic products from the tuff cone; D: juvenile clast from the lower dacitic sequence; E, F, G: vitric clasts from the surtseyan-like deposits (sequence II); H: basaltic ash flow from sequence III. I, J, K: pre-historic basalt from the caldera floor (I), and historic lava flows of 1914 (J) and 1988 (K).

3), 10–25 m thick, consists mainly of grey to blueish ash flow deposits, almost free of xenoliths in beds a few meters thick. The highly to extremely vesicular (60–90%) "dry" sideromelane droplets (Fig. 5C) and pumiceous lapilli are basaltic (analysis H, Table 1). Translucent ash particles show fragmentation after cooling but no reworking after deposition; other grains have a smooth appearance.

Sequence IV. Sequence IV of the APS belongs to the last volcanic events before the caldera formation. On the south slope of the cone, strombolian deposits, basaltic in composition,

Fig. 5. (A and B) Microphotographs of vitric clasts of the surtseyan-like beds (sequence II of the Ambrym Pyroclastic Series). (A) Blocky clast in granular matrix with palagonite. (B) Poorly vesicular clast. (C) SEM photograph of highly vesicular sideromelane droplet (1 mm). From sequence III (basaltic ash flow deposits; analysis column H, Table 1).

constitute this sequence. Their origin is the Woosantapaliplip vent, located on the caldera rim (Fig. 2). Here, the thickness of these deposits reaches 200 m.

On the north side of the cone, viscous lavas, 20–25 m thick, basaltic andesite in composition, overly the APS. They extruded on the caldera edge and flowed downward as far as Bogorfan Bay (location Fig. 2), forming a 2-km-wide large lava tongue. Near the vent, part of these flows remained in the caldera and have been intersected by the collapse (Fig. 7).

Geochemistry of tuffs

Most juvenile clasts are aphyric. 137 microprobe analyses of juvenile glasses from the APS show compositions ranging from medium-K calc-alkaline basalt to dacite. A histogram for SiO_2 content (Fig. 6) clearly shows 3 peaks at 50% SiO2 (basalts), 54% (basaltic andesites) and 66% (dacites). Five whole-rock analyses from these clasts are also reported Table 1 (columns D to H). Dacitic compositions are restricted to products of sequence I, whereas basalts and subordinated basaltic andesites constitute the juvenile material of sequences II, III and IV, i.e. the main volume of the APS deposits. A few juvenile clasts contain olivine (Fo_{72-82}), calcic pyroxene and plagioclase (bytownite).

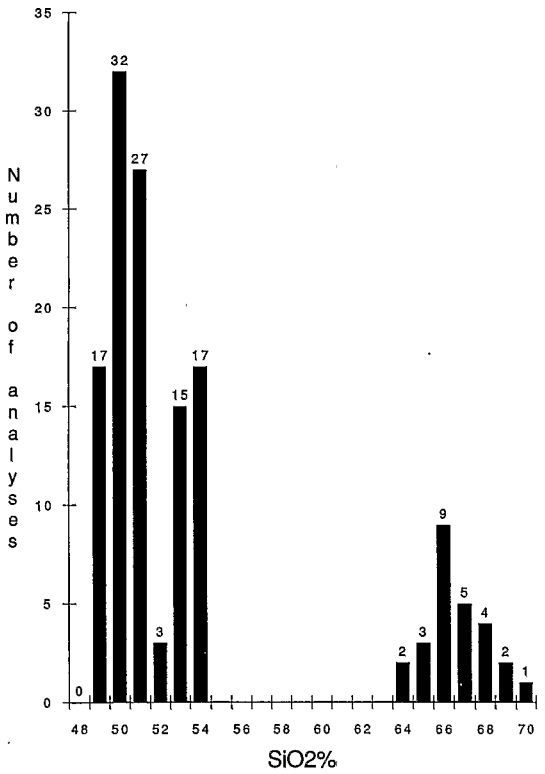

Fig. 6. SiO_2 histogram of 137 microprobe analyses of vitric clasts from the syn-caldera Ambrym Pyroclastic Series (APS). Class interval: 1%. As example, for SiO_2 = 50%, 32 analyses from 49.5 to 50.5.

Post-caldera volcanism

Within the caldera, the major vents occur along fissures oriented N 105°E and appear as scoria cones, maars and fissures that fed lava flows from the lower flanks of the volcano. Post-caldera activity, dominantly from the Marum (1270 m) and Benbow (1160 m) cones (Fig. 7), has infilled the depression and is responsible for a gently eastward-sloping caldera floor from 700 to 550 m of altitude. Ambrym has had a large number of historical eruptions, e.g., in 1888, 1894, 1913–14, 1929, 1937, 1942, 1952–53, etc (Fisher, 1957; Williams and Warden, 1964), the latest being in 1989 (Eissen et al., 1991). Episodic lava lakes in the craters of Benbow and Marum drain out as basaltic lava flows onto the caldera floor. Magma in the conduit is also frequently ejected as ash and scoria falls, which mantle the caldera and the west part of the volcano. Figure 7 shows the distribution of the main historic and prehistoric lava flows as well as the presence in the eastern part of the caldera of a recent maar (Lewolembwi crater) surrounded by a 2-km-wide tuff ring. Older coalescent structures of the same type are infilled by the 1986 lava flows. In September 1990, the main activity was concentrated in the Mbwelesu, Niri Mbwelesu and Niri Mbwelesu Taten craters. Three analyses representative of the post-cald-

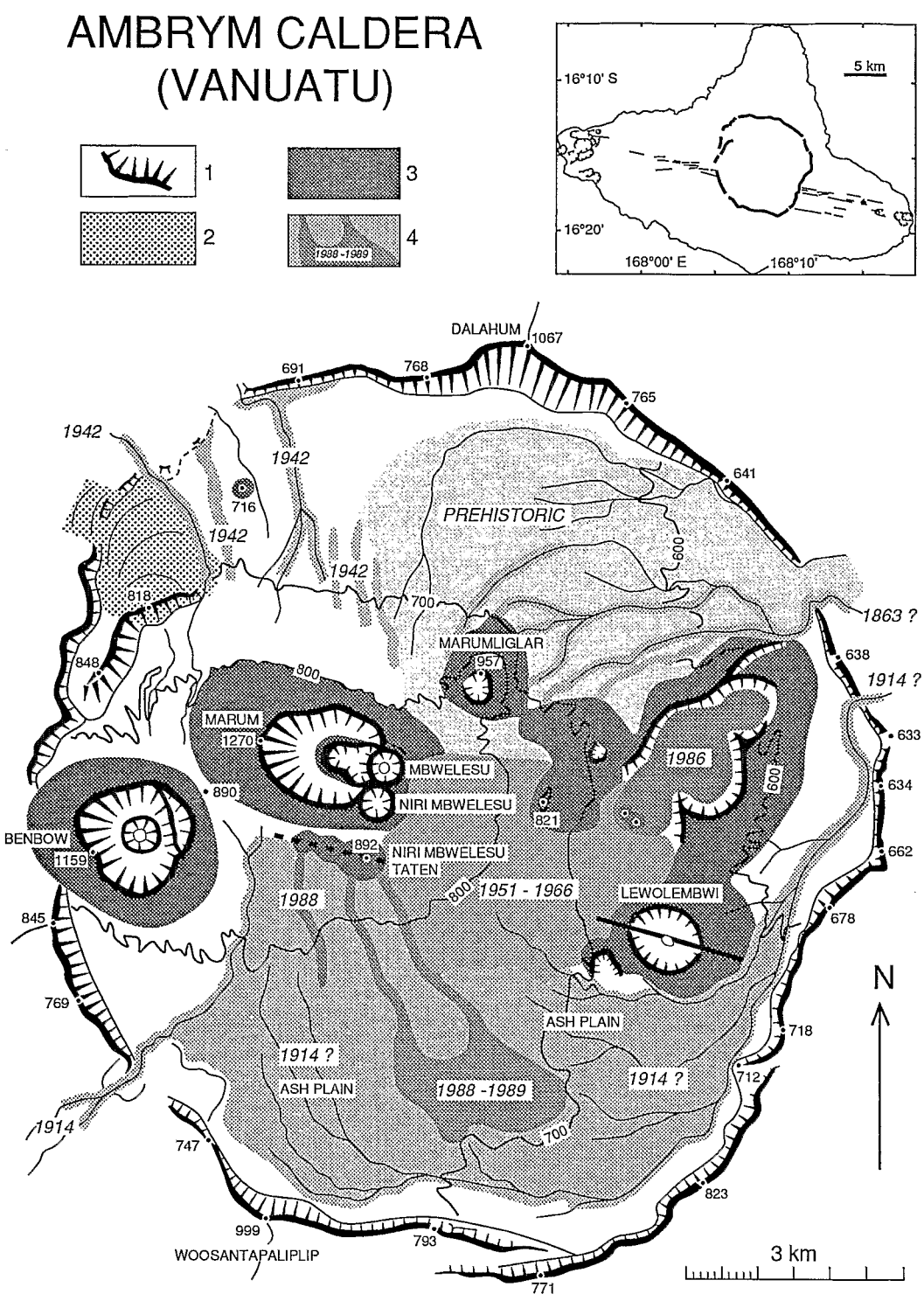

Fig. 7. Sketch volcanologic map of the caldera. *1*=caldera scarp; *2*=Bogorfan basaltic andesite viscous lava flow; *3*=volcanic cones; *4*=pre-historic and historic lava flows. (Drawing by J. Butscher)

era basaltic activity are reported in Table 1 (see also Robin et al., 1991).

Discussion

Structure of the volcano

The APS tuffs dip at similar angles (10–20°) to the present upper slopes surrounding the caldera, above a break of slope at about 6 km away from the caldera rim (Fig. 8). Since the dips of the underlying fluid lava flows are constant (2–3°), the APS thickens towards the caldera, as observed on the southern flank, along the track from Lalinda to the caldera edge. In addition, no lava flows have been encountered in the caldera wall, the average slope of which (≈40°) is relatively low and does not agree with a piston-like collapse caldera. Thus, Ambrym differs from other oceanic volcanoes whose slopes generally expose piles of lava flows with minor interstratified tuffs (Macdonald et al, 1983; Peterson and Moore, 1987; Walker, 1990). *The structure of the edifice is that of a shield lava volcano, overlain by an uncommonly large tuff cone, the inner part of which has subsided.* Along the caldera fault, the height of the buried pre-caldera edifice is probably 200 to 300 m, except on the northeastern side where it is very low (about 100 m). This suggests a thickness ranging from 200 to 450 m for the APS deposit near the caldera edge (up to 600 m at Woosantapaliplip Peak) and a volume between 60 and 80 km^3 (at least 20 km^3 Dense Rock Equivalent).

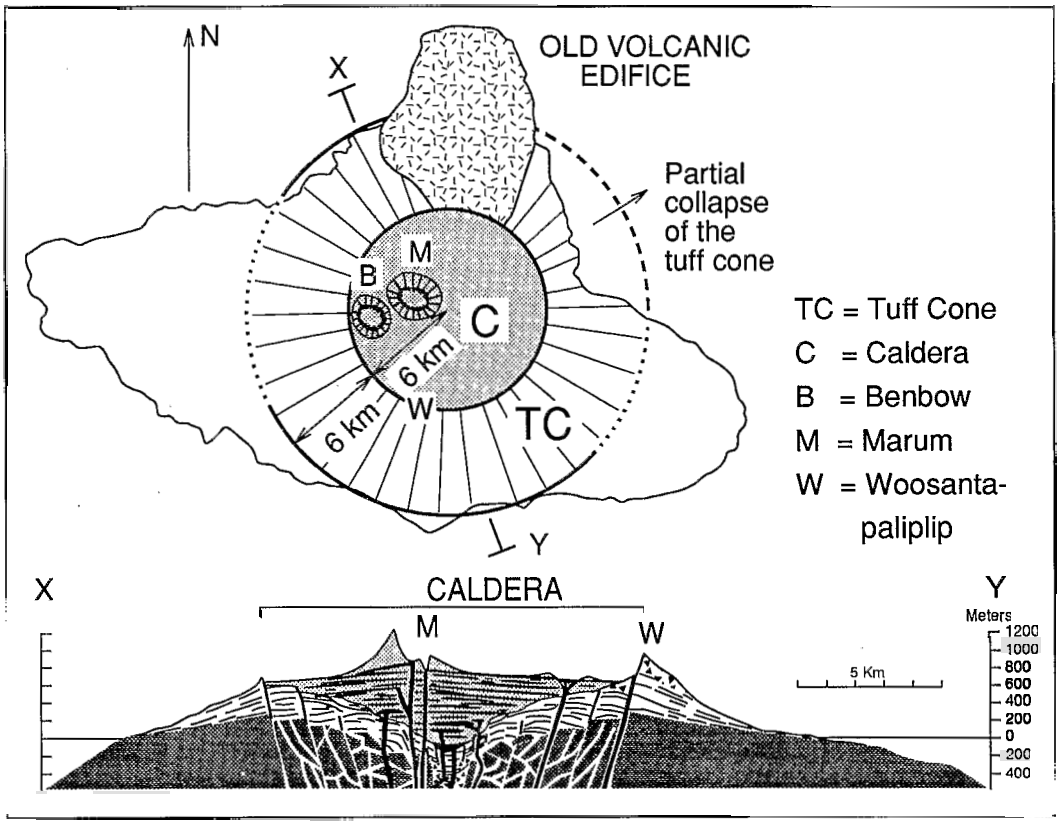

Fig. 8. Sketch map of Ambrym and inferred cross-section (X–Y) showing the basal edifice (dark grey), the tuff cone (white) and the post-caldera volcanics (light grey). Vertical exageration ×3.

Age of the caldera

The caldera is morphologically well preserved (Figs. 2, 7). The perfect, nearly circular, ring structure is marked by a continuous scarp a few tens of meters up to 450 m high in two points, the Dalahum and Woosantaliplip Peaks. As noted by MacCall et al. (1970), the scarps are only mildly scalloped and gullied by erosion, a noteworthy feature in this tropical environment. This agrees with the young ^{14}C ages (less than 2,000 years) proposed by these authors.

Relationship between the APS and the caldera formation

The very fragile nature of the vesiculated clasts and shards which compose the APS, the sorting of the beds and the preservation of accretionary lapilli indicate that these deposits are not reworked materials. The large volume of the pyroclastic edifice does not agree with the relatively small volume of a tuff cone (Mertes, 1983), the central depression of which would correspond to a simple crater enlarged by explosive coring.

By the volume of basalt released, the pyroclastic event at the origin of the APS is drastically different from those which led to the deposit of tuffs associated with a caldera in other large basaltic volcanoes, as the 1790 Keanakakoi ash member at Kilauea (Swanson and Christiansen, 1973; MacPhie et al., 1990). The eruption of the Keanakakoi tuff (0.1 km^3) produced only minor shape modification of the Kilauea summit caldera. The 1886 eruption at Tarawera led to basaltic Plinian deposits of greater volume (Walker et al., 1984), but the products were emitted along a linear fissure and are not associated with a collapse. At Masaya (Nicaragua), caldera collapse apparently formed in response to large scale pyroclastic eruptions of basaltic magma, including ignimbrites and surges (Williams, 1983a,b; Bice, 1985). This caldera seems the only known example which resembles, in terms of mechanisms of producing Plinian basaltic eruptions, the large tuff cone of Ambrym. Vertical continuity, volume, large extent and the range in composition of the juvenile clasts are strong arguments favouring the thesis that the APS products erupted during a major pyroclastic event related to the emptying of a chemically zoned magmatic chamber, mainly basaltic in composition.

Since the very early studies of the formation of calderas, the respective roles of explosive coring *versus* collapse have been debated (see Scandone, 1990, and McBirney, 1990 for reviews of this subject). At Ambrym, the problem is even more complicated for three reasons:

(a) First, widely-dispersed plinian-like basaltic deposits are rare, and basalts are generally considered unable to provoke large Plinian eruptions. To lead to the emptying of a basaltic reservoir, intervention of external water is likely to occur at the roof of the magma chamber.

(b) Second, the presence of a gigantic tuff cone which exposes alternate ash flow deposits and rhythmic deposits typical of maar and surtseyan eruptions, as well as the large size of the caldera *imply a combination of both explosive coring and collapse.*

(c) Third, although collapse probably began when sequence I of the APS erupted (see below the model proposed), products of sequences II to IV also are affected by subsidence. To lead to the construction of sequence II or to that of the Woosantapaliplip cone (sequence IV), the pyroclastic eruption at the origin of the APS must have been an eruption the duration of which lasted several months or even years, and several subsidence stages probably occurred. It is notable that the composite lower sequence of dacitic ignimbrites exposes an intermediate series of phreatomagmatic fallout layers and, therefore, was emitted during a lengthy event.

Tentative model of caldera formation

The structure of the volcano, the distribution and volume of pyroclastics, and their relationships with the ring structure show that eruption of the APS is responsible for the caldera formation. Moreover, the interpretation of successive sequences which constitute the APS provide evidence relating to the timing of water entrance into the magma system.

(1) Eruption of sequence I: earlier caldera collapse

The volume of the dacitic pyroclastic flows from sequence I cannot be estimated, due to their unknown extent below sealevel. Based on the thickness of deposits, they represent a major plinian phase which probably occurred after a long-lasting period of quiescence, allowing magmatic differentiation. Their eruption led to collapse in the summit area of the volcano. The large percentage of accidental clasts from the basal volcano incorporated in the coarse layers (Fig. 3) is an argument in favour of collapse of the roof into the magma reservoir and enlargement of the vent during the eruption.

Energy released by expansion of magmatic gases may have been sufficient to initiate the eruption. Nevertheless, the lower dacitic pyroclastic flow deposits from sequence I show phreatomagmatic features, as evidenced by water-induced fragmentation of glass, the vesicularity indices of which are low, and also the broad vesicularity range. These deposits are followed immediately by typical phreatomagmatic deposits such as those shown in Figure 4C. Thus, magma/water interaction is important even during the earliest stages of the eruption.

The formation of a caldera subsequent to eruption of sequence I does not preclude the possibility of a pre-existing caldera of the Kilauea type at the top of the shield volcano, and a lake within such a structure could explain the phreatomagmatic processes in this sequence. Introduction of sea water into the flat edifice represents an alternative hypothesis to explain magma/water interaction; this would be related to regional doming and fracturing following uprise of a large magma body to shallow depth and/or seismic events affecting the N 105°E fracture zone.

(2) Construction of the tuff cone as collapse enlarges

The products of sequence II resemble those erupted in Surtsey in 1960 (Thorarinsson et al., 1964; Walker and Croasdale, 1972; Kokelaar, 1983, 1986). The thick ring of accumulated vitric tuffs, with radial dips, and the textures of the clasts, are consistent with a hydroclastic origin. As juvenile clasts have moderate to high vesicularity, we propose a phreatomagmatic explosive mode of fragmentation for an already vesiculated erupting basaltic magma (Cas and Wright, 1987; Cas et al., 1989). The accretionary lapilli beds are also diagnostic of a wet eruptive column of extremely disaggregated material. It was at this stage of the eruption that sea water probably entered the upper levels of the magmatic reservoir.

Although the ash deposits of sequence III include noncarbonized plant fragments, the flowage of these deposits and the surface features of shards indicate pyroclastic origin and an emplacement similar to that of ignimbrites. The rounded surface of some of the ash results from chipping and pitting during transport in the flow. The high vesicularity of the fragments results from decompression and expansion of magmatic volatiles, and fast cooling of the ash flows suggests interaction between magma and external water. At this stage, explosive eruptions may have been catalyzed by water, but to a lesser extent than in the preceding sequence II.

During this second phase of the eruption, both explosive coring and collapse processes occur. Since surtseyan-like deposits are likely to occur in a centered eruption, and as the subsequent Woosantapaliplip deposits and Bogorfan Bay lava flows from sequence IV origi-

nated near the ring fracture, an enlargement of the collapse during eruption of sequences II and III may have occurred as the cone was growing (Fig. 8). Temporal continuity in the eruption is indicated by the grading from deposits of sequences I to II and then to III. Nevertheless, a question which remains to be solved is the duration of this phase. The eruption probably lasted months or even a few years.

(3) Final phase: eruptive vents on the ring fracture

Finally, the construction of the Woosantapaliplip strombolian cone and the eruption of lavas which flowed towards Bogorfan Bay confirm a decreasing role of water. These formations are affected by the final collapse. Probably other vents opened when the caldera enlarged, but are now buried by post-caldera volcanics.

Thus, in terms of eruptive dynamics, the interpretation of the APS deposits imply intervention of external water and both explosive and collapse mechanisms. The eruptive event commences with eruption of the dacites from sequence I and continues with the subsequent basaltic eruptions after penetration of water into the shallow chamber. This mechanism leads to caldera collapse by evacuation of the large, mainly basaltic chamber at shallow depth below the volcano. This model, different from those generally considered for both large continental and Hawaiian calderas, explains the original structure of the Ambrym basaltic complex, half-way between a large caldera and an exceptionally large tuff cone.

Acknowledgments

This work was financially supported by ORSTOM UR 1F and French Foreign Affairs Ministry (MAE). We thank C. Picard (Université Française du Pacifique, Nouméa) and C. Douglas for useful participation during fieldwork. We are also grateful to Katharine Cashman, University of Oregon, and to Anthony Crawford, University of Tasmania, for constructive and helpful comments of a first version. Prof. P.M. Vincent, S. Self and D.A. Swanson reviewed the manuscript. C. Mortimer, Director of the Department of Geology, Mines and Rural Water Supply of Vanuatu, and C. Reichenfeld, Director of the ORSTOM Centre of Port-Vila, constantly supported our investigations.

References

Batiza, R., Fornari, D.J., Vanko, D.A. and Lonsdale, P., 1984. Craters, calderas, and hyaloclastites on young Pacific seamounts. J. Geophys. Res., 89(B10): 8371–8390.

Bice, D.C., 1985. Quaternary volcanic stratigraphy of Managua, Nicaragua: correlation and source assignement for multiple overlapping plinian deposits. Geol. Soc. Am. Bull., 96: 553–566.

Cas, R.A.F. and Wright, J.V., 1987. Volcanic Successions: Modern and Ancient. A Geological Approach to Processes, Products and Successions. Allen & Unwin, London, 528 pp.

Cas, R.A.F., Landis, C.A. and Fordyce, R.E., 1989. A monogenetic, Surtla-type, Surtseyan volcano from the Eocene–Oligocene Waiareka–Deborah volcanics, Otago, New Zealand: a model. Bull. Volcanol., 51: 281–298.

Chase, T.E. and Seekins, B.A., 1988. Submarine topography of the Vanuatu and southeastern Solomon Islands regions. In: H.G. Greene and F.L. Wong (Editors), Geology and Offshore Resources of Pacific Island Arcs – Vanuatu Region. Circum-Pacific Council Energy Miner. Resour., Earth Sci. Ser., 8: 35–36.

Eissen, J.-Ph., Blot, C. and Louat, R., 1991. Chronology of the historic volcanic activity of the New Hebrides island arc from 1595 to 1991. Report, ORSTOM, Nouméa, New Caledonia, 69 pp.

Fisher, N.H., 1957. Catalogue of the active volcanoes of the world including solfatara fields, Part V, Melanesia. Int. Volcanol. Assoc., Naples, 106 pp.

Fisher, R.V. and Smincke, H.-U., 1984. Pyroclastic Rocks. Springer, Berlin-Heidelberg-New York-Tokyo, 472 pp.

Houghton, B.F. and Wilson, C.J.N. 1989. A vesicularity index for pyroclastic deposits. Bull. Volcanol., 51: 451–462.

Kokelaar, B.P., 1983. The mechanism of surtseyan eruption. J. Geol. Soc. London, 140: 939–944.

Kokelaar, B.P., 1986. Magma–water interactions in subaqueous and emergent basaltic volcanism. Bull. Volcanol., 48: 275–289.

MacCall, G.J.H., LeMaitre, R.W., Malahoff, A., Robinson, G.P. and Stephenson, P.J., 1970. The geology and

geophysics of the Ambrym Caldera, New Hebrides. Bull. Volcanol., 34: 681–696.
MacDonald, G.A., Abbott, A.T. and Peterson, F.L., 1983. Volcanoes in the Sea, 2nd ed., University of Hawaii Press, Honolulu.
Macfarlane, A. (Editor), 1976. Geology of Pentecost and Ambrym, 1: 100,000 New Hebrides Geol. Surv. Sheet 6, Geol. Surv. Dept., Port Vila, New Hebrides.
MacPhie, J., Walker, G.P.L. and Christiansen, R.L., 1990. Phreatomagmatic and phreatic fall and surge deposits from explosions at Kilauea volcano, Hawaii, 1790 A.D.: Keanakakoi Ash Member. Bull. Volcanol., 52: 334–354.
McBirney, A.R., 1990. An historical note on the origin of calderas. J. Volcanol. Geotherm. Res., 42: 303–306.
Mertes, H., 1983. Aufbau und Genese des Westeifeler Vulcanfeldes. Bochumer Geol. Geotechn. Arb., 9: 1–415.
Peterson, D.W. and Moore, R.B., 1987. Volcanism in Hawaii. Geologic history and evolution of geologic concepts, island of Hawaii. U.S. Geol. Surv., Prof. Pap., 1350: 149–189.
Quantin, P., 1978. Archipel des Nouvelles-Hébrides: atlas des sols et de quelques données du milieu, 18 feuilles et 11 notices, ORSTOM, Paris.
Robin, C., Monzier, M., Eissen, J.P., Picard, C. and Camus, G., 1991. Coexistence de lignées HK et MK dans les pyroclastites associées à la caldéra d'Ambrym (Vanuatu, Arc des Nouvelles Hébrides). C. R. Acad Sci., 313 sér. II: 1425–1432.
Scandone, R., 1990. Chaotic collapse of calderas. J. Volcanol. Geotherm. Res., 42: 285–302.
Swanson, D.A. and Christiansen, R.L., 1973. Tragic base surge in 1790 at Kilauea volcano. Geology, 1: 83–86.
Thorarinsson, S., Einarsson, Th., Sigvaldason, G.E. and Elisson, G., 1964. The submarine eruption off the Westmann Islands 1963–64. Bull. Volcanol., 27: 1–11.
Walker, G.P.L., 1990. Geology and Volcanology of the Hawaiian Islands. Pac. Sci., 44(4): 315–347.
Walker, G.P.L. and Croasdale, R., 1972. Characteristics of some basaltic pyroclastics. Bull. Volcanol., 35: 303–317.
Walker, G.P.L., Self, S., Wilson, L., 1984. Tarawera 1886, New Zealand — A basaltic plinian fissure eruption. J. Volcanol. Geotherm. Res., 21: 61–78.
Williams, C.E.F. and Warden, A.J., 1964. Progress report of the Geological Survey for 1959–1962. New Hebrides Geol. Surv. Rept., Port Vila, New Hebrides, pp. 75.
Williams, S.N., 1983a. Geology and eruptive mechanisms of Masaya Caldera complex, Nicaragua. PhD thesis, Darmouth College, Hannover, NH, 169 pp.
Williams, S.N., 1983b. Plinian airfall deposits of basaltic composition. Geology, 11: 211–214.